

# Quantum coherent saturable absorption for mid-infrared ultra-short pulses

Muhammad Anisuzzaman Talukder<sup>1,2,\*</sup> and Curtis R. Menyuk<sup>2</sup>

<sup>1</sup>Department of Electrical and Electronic Engineering,  
Bangladesh University of Engineering and Technology,  
Dhaka 1000, Bangladesh

<sup>2</sup>Department of Computer Science and Electrical Engineering,  
University of Maryland, Baltimore County,  
1000 Hilltop Circle, Baltimore, MD 21250, USA

[\\*anis@eee.buet.ac.bd](mailto:anis@eee.buet.ac.bd)

**Abstract:** We theoretically show that quantum coherent saturable absorption can be used to obtain ultra-short pulses from mid-infrared quantum cascade lasers (QCLs). In this proposal, quantum cascade structures are processed as two electrically isolated sections. The two sections will be biased with two different voltages so that one of the sections produces gain as is done in typical QCLs, while the other produces quantum coherent resonant absorption for the propagating waves. The quantum coherent absorbing section is saturable and favors the generation of ultra-short pulses. We find that stable ultra-short pulses on the order of  $\sim 100$  ps are created from a two-section QCL when the pumping in the gain and absorbing sections remains within critical limits. The intensity and the duration of the stable pulses can be significantly varied when the pumping in the gain and absorbing sections and the length of the gain and absorbing sections are varied.

© 2014 Optical Society of America

**OCIS codes:** (140.5965) Semiconductor lasers, quantum cascade; (140.7090) Ultrafast lasers.

---

## References and links

1. R. Paiella, F. Capasso, C. Gmachl, D. L. Sivco, J. N. Baillargeon, A. L. Hutchinson, A. Y. Cho, and H. C. Liu, "Self-mode-locking of quantum cascade lasers with giant ultrafast optical nonlinearities," *Science* **290**, 1739–1742 (2000).
2. R. Paiella, F. Capasso, C. Gmachl, H. Y. Hwang, D. L. Sivco, A. L. Hutchinson, A. Y. Cho, and H. C. Liu, "Monolithic active mode locking of quantum cascade lasers," *Appl. Phys. Lett.* **77**, 169–171 (2000).
3. A. Soibel, F. Capasso, C. Gmachl, M. L. Peabody, A. M. Sergent, R. Paiella, D. L. Sivco, A. Y. Cho, and H. C. Liu, "Stability of pulse emission and enhancement of intracavity second-harmonic generation in self-mode-locked quantum cascade lasers," *IEEE J. Quantum Electron.* **40**, 197–204 (2004).
4. A. Soibel, F. Capasso, C. Gmachl, M. L. Peabody, A. M. Sergent, R. Paiella, H. Y. Hwang, D. L. Sivco, A. Y. Cho, H. C. Liu, C. Jirauschek, and F. X. Kärtner, "Active mode locking of broadband quantum cascade lasers," *IEEE J. Quantum Electron.* **40**, 844–851 (2004).
5. C. Y. Wang, L. Kuznetsova, V. M. Gkortsas, L. Diehl, F. X. Kärtner, M. A. Belkin, A. Belyanin, X. Li, D. Ham, H. Schneider, P. Grant, C. Y. Song, S. Haffouz, Z. R. Wasilewski, H. C. Liu, and F. Capasso, "Mode-locked pulses from mid-infrared quantum cascade lasers," *Opt. Express* **17**, 12929–12943 (2009).
6. A. K. Wójcik, P. Malara, R. Blanchard, T. S. Mansuripur, F. Capasso, and A. Belyanin, "Generation of picosecond pulses and frequency combs in actively mode locked external ring cavity quantum cascade lasers," *Appl. Phys. Lett.* **103**, 231102 (2013).
7. S. Barbieri, M. Ravora, P. Gellie, G. Santarelli, C. Manquest, C. Sirtori, S. P. Khanna, E. H. Linfield, and A. Giles Davies, "Coherent sampling of active mode-locked terahertz quantum cascade lasers and frequency synthesis," *Nat. Photonics* **5**, 306–313 (2011).

8. A. Hugi, G. Villares, S. Blaser, H. C. Liu, and J. Faist, "Mid-infrared frequency comb based on a quantum cascade laser," *Nature* **492**, 229–233 (2012).
9. Y. Wang, M. G. Soskind, W. Wang, and G. Wysocki, "High-resolution multi-heterodyne spectroscopy based on Fabry-Perot quantum cascade laser," *Appl. Phys. Lett.* **104**, 031114 (2014).
10. J. B. Khurgin, Y. Dikmelik, A. Hugi, and J. Faist, "Coherent frequency combs produced by self frequency modulation in quantum cascade lasers," *Appl. Phys. Lett.* **104**, 081118 (2014).
11. D. Burghoff, T.-Y. Kao, N. Han, C. W. I. Chan, X. Cai, Y. Yang, D. J. Hayton, J.-R. Gao, J. L. Reno, and Q. Hu, "Terahertz laser frequency combs," *Nat. Photonics* **8**, 462–467 (2014).
12. V. M. Gkortsas, C. Wang, L. Kuznetsova, L. Diehl, A. Gordon, C. Jirauschek, M. A. Belkin, A. Belyanin, F. Capasso, and F. X. Kärtner, "Dynamics of actively mode-locked quantum cascade lasers," *Opt. Express* **18**, 13616–13630 (2010).
13. A. Gordon, C. Y. Wang, L. Diehl, F. X. Kärtner, A. Belyanin, D. Bour, S. Corzine, G. Höfler, H. C. Liu, H. Schneider, T. Maier, M. Troccoli, J. Faist, and F. Capasso, "Multimode regimes in quantum cascade lasers: From coherent instabilities to spatial hole burning," *Phys. Rev. A* **77**, 053804 (2008).
14. C. R. Menyuk and M. A. Talukder, "Self-induced transparency modelocking of quantum cascade lasers," *Phys. Rev. Lett.* **102**, 023903 (2009).
15. M. A. Talukder and C. R. Menyuk, "Analytical and computational study of self-induced transparency modelocking in quantum cascade lasers," *Phys. Rev. A* **79**, 063841 (2009).
16. S. S. Shimu, A. Docherty, M. A. Talukder, and C. R. Menyuk, "Suppression of spatial hole burning and pulse stabilization for actively modelocked quantum cascade lasers using quantum coherent absorption," *J. Appl. Phys.* **113**, 053106 (2013).
17. R. W. Boyd, *Nonlinear Optics*, 2nd ed. (Academic Press, 2003).
18. R. Terazzi and J. Faist, "A density matrix model of transport and radiation in quantum cascade lasers," *New J. Phys.* **12**, 033045 (2010).
19. M. A. Talukder and C. R. Menyuk, "Temperature-dependent coherent carrier transport in quantum cascade lasers," *New J. Phys.* **13**, 083027 (2011).
20. M. A. Talukder, "Modeling of gain recovery of quantum cascade lasers," *J. Appl. Phys.* **109**, 033104 (2011).
21. M. A. Talukder and C. R. Menyuk, "Calculation of the microscopic parameters of a self-induced transparency modelocked quantum cascade laser," *Opt. Comm.* **295**, 115–118 (2013).
22. S. L. McCall and E. L. Hahn, "Self-induced transparency," *Phys. Rev.* **183**, 457–489 (1969).
23. I. M. Asher, "Experimental investigation of self-induced transparency and and pulse delay in Ruby," *Phys. Rev. A* **5**, 349–355 (1972).
24. M. A. Talukder and C. R. Menyuk, "Self-induced transparency modelocking of quantum cascade lasers in the presence of saturable nonlinearity and group velocity dispersion," *Opt. Express* **18**, 5639–5653 (2010).

---

## 1. Introduction

The realization of mid-infrared short pulses from compact semiconductor light sources, i.e., quantum cascade lasers (QCLs) has been a challenge for last one and a half decades. Despite repeated attempts, there has only been limited success [1–7]. Recently, it has been shown that QCLs can be used to produce frequency combs using four-wave mixing or self frequency modulation [8–11]. However, there has been no experimental demonstration of passive modelocking to date, and although active modelocking has been experimentally demonstrated, pulses are not stable when the laser operates even marginally above the threshold, but undergo at least a slow evolution [5, 12]. It has been shown that the very fast gain recovery of QCLs favors the growth of continuous waves when the input current is above the threshold that is required for lasing [12]. Short pulses cannot be created as the gain recovers within the duration of the pulse, so that the tail of the pulse experiences more gain than does its peak. Additionally, the fast gain recovery leads to spatial hole-burning. Although the spatial hole-burning leads to the excitation of a large number of longitudinal modes, these modes cannot be phase-locked due to the rapid time evolution of the hole-burning [12, 13].

It has been theoretically shown that the self-induced transparency (SIT) effect can be used to modelock QCLs if absorbing periods are grown interleaved with gain periods [14, 15]. SIT modelocked QCLs produce stable pulses on the order of  $\sim 100$  fs duration over a broad parameter regime. The key way in which SIT modelocking differs from standard modelocking is that it is no longer necessary to have a gain bandwidth that is equal to the inverse pulse duration [14].

However, these lasers do not self-start. Structures with interleaved gain and absorbing periods can also be used for active-SIT modelocking to increase the stability regime and self-start the laser [16]. It has been shown that active-SIT-modelocked QCLs can produce stable pulses on the order of  $\sim 1$  ps. However, the success of both of these approaches requires the gain and absorbing periods to be in resonance and the gain and absorption parameters to be within limiting values. In a structure where gain and absorbing periods are interleaved, the pump parameters cannot be controlled individually, which makes it difficult to realize the mid-infrared pulses experimentally.

In this work, we present a way to create ultra-short pulses from QCLs using distributed gain and absorption along the axial cavity length. The cascaded quantum heterostructure will be designed so that it becomes a gain medium at one bias voltage and a coherent resonant absorbing medium at another bias voltage. The cavity will be processed into two electrically isolated sections so that different bias voltages can be applied to distribute gain and resonant absorption along the cavity length. The resonant absorbing section behaves like a saturable absorber; it absorbs continuous waves and suppresses the spatial hole-burning. We find that this scheme lets the laser self-start from random quantum noise and produces ultrashort stable pulses with durations that can be shorter than 100 fs. The pulse duration can be changed by independently varying the bias of the gain and absorbing sections.

The remaining of the paper is organized as follows: In Sec. 2, we present the physical concept of the proposed approach. We also present the Maxwell-Bloch equations that describe the light propagation and light-medium interaction in the cavity, and we derive the critical pumping limits for stable ultra-short pulses. In Sec. 3, we present results that are obtained by solving the Maxwell-Bloch equations for a two-section QCL. In Sec. 4, we present our conclusions.

## 2. Theoretical model

A schematic illustration of the proposed two-section QCL is shown in Fig. 1, along with two-level representations of the gain and absorbing sections. The quantum layers are grown in the vertical direction and are the same throughout the cavity in the longitudinal direction. However, the cavity is processed into two electrically isolated sections by etching the cladding layers deposited on the active region as is done for actively modelocked lasers [12]. The longer section is biased with a voltage  $V_1$ , so that the upper level is pumped by  $\lambda_g$ . The longer section is inverted in equilibrium and produces gain as in typical QCLs. By contrast, the smaller section is biased with a voltage  $V_2$ , so that the lower level is pumped by  $\lambda_a$ . The smaller section is uninverted in equilibrium and produces resonant absorption as the light emitted from the gain section propagates through it. The current going into the gain and absorbing sections determines the resonant frequency in each of the sections as well as respectively the gain and quantum coherent absorption. The quantum coherent absorption acts as a saturable absorber, absorbing continuous waves while allowing pulses that are half a Rabi oscillation in duration to pass through. In SIT modelocked QCLs, gain and absorption frequencies must be in resonance to within the linewidths of both [15]. By contrast, SIT modelocking will still work over a broad range of ratios of gain to absorption as long as close to zero detuning is maintained. An advantage of our current proposal is that it is possible to independently tune the biases in the gain and absorbing sections, so that the ratio of the gain and absorption can be optimized, while the detuning can be made close to zero. It is possible to create ultra-short pulses over a broad range of gain and absorption [15]. If the gain becomes too small relative to the absorption, then the pulses are absorbed; if the gain becomes too large relative to the absorption, then multiple pulses are produced.



length not including mirror losses,  $\lambda_x$  denotes the pump parameter,  $D$  denotes the diffusion coefficient,  $d_x$  denotes the dipole matrix element of the laser transition, and  $k$  denotes the wave number associated with the optical resonance frequency. We may write  $k = \omega n/c$ , where  $\omega$  denotes the angular frequency of the electric field.

For simulation purposes, we normalize the field, polarization, inversion, and inversion grating using the transformations

$$\tilde{E}_{\pm} = \frac{d_g}{\hbar} E_{\pm}, \quad (3a)$$

$$\tilde{\eta}_{g,a\pm} = \frac{kN_{g,a}\Gamma_{g,a}d_{g,a}^2}{\hbar\epsilon_0 n^2} \eta_{g,a\pm}, \quad (3b)$$

$$\tilde{\Delta}_{0g,a} = \frac{kN_{g,a}\Gamma_{g,a}d_{g,a}^2}{\hbar\epsilon_0 n^2} \Delta_{0g,a}, \quad (3c)$$

$$\tilde{\Delta}_{2g,a} = \frac{kN_{g,a}\Gamma_{g,a}d_{g,a}^2}{\hbar\epsilon_0 n^2} \Delta_{2g,a}, \quad (3d)$$

$$\tilde{\lambda}_{g,a} = \frac{kN_{g,a}\Gamma_{g,a}d_{g,a}^2}{\hbar\epsilon_0 n^2} \lambda_{g,a}. \quad (3e)$$

Using the normalizations given in Eq. (3), the coupled Maxwell-Bloch equations for the gain section in Eq. (1) can be written as

$$\frac{n}{c} \frac{\partial \tilde{E}_{\pm}}{\partial t} = \mp \frac{\partial \tilde{E}_{\pm}}{\partial z} - i\tilde{\eta}_{g\pm} - l\tilde{E}_{\pm}, \quad (4a)$$

$$\frac{\partial \tilde{\eta}_{g\pm}}{\partial t} = \frac{i}{2} (\tilde{\Delta}_{0g}\tilde{E}_{\pm} + \tilde{\Delta}_{2g}^{\mp}\tilde{E}_{\mp}) - \frac{\tilde{\eta}_{g\pm}}{T_{2g}}, \quad (4b)$$

$$\frac{\partial \tilde{\Delta}_{0g}}{\partial t} = \tilde{\lambda}_g + i(\tilde{E}_+^* \tilde{\eta}_{g+} + \tilde{E}_-^* \tilde{\eta}_{g-} - \text{c.c.}) - \frac{\tilde{\Delta}_{0g}}{T_{1g}}, \quad (4c)$$

$$\frac{\partial \tilde{\Delta}_{2g}^{\pm}}{\partial t} = i(\tilde{E}_{\pm}^* \tilde{\eta}_{g\mp} - \tilde{E}_{\mp} \tilde{\eta}_{g\pm}^*) - \left( \frac{1}{T_{1g}} + 4k^2 D \right) \tilde{\Delta}_{2g}^{\pm}, \quad (4d)$$

and the coupled Maxwell-Bloch equations for the absorbing section in Eq. (2) can be written as

$$\frac{n}{c} \frac{\partial \tilde{E}_{\pm}}{\partial t} = \mp \frac{\partial \tilde{E}_{\pm}}{\partial z} - i\frac{d_a}{d_g} \tilde{\eta}_{a\pm} - l\tilde{E}_{\pm}, \quad (5a)$$

$$\frac{\partial \tilde{\eta}_{a\pm}}{\partial t} = \frac{i}{2} \frac{d_a}{d_g} (\tilde{\Delta}_{0a}\tilde{E}_{\pm} + \tilde{\Delta}_{2a}^{\mp}\tilde{E}_{\mp}) - \frac{\tilde{\eta}_{a\pm}}{T_{2a}}, \quad (5b)$$

$$\frac{\partial \tilde{\Delta}_{0a}}{\partial t} = \tilde{\lambda}_a + i\frac{d_a}{d_g} (\tilde{E}_+^* \tilde{\eta}_{a+} + \tilde{E}_-^* \tilde{\eta}_{a-} - \text{c.c.}) - \frac{\tilde{\Delta}_{0a}}{T_{1a}}, \quad (5c)$$

$$\frac{\partial \tilde{\Delta}_{2a}^{\pm}}{\partial t} = i\frac{d_a}{d_g} (\tilde{E}_{\pm}^* \tilde{\eta}_{a\mp} - \tilde{E}_{\mp} \tilde{\eta}_{a\pm}^*) - \left( \frac{1}{T_{1a}} + 4k^2 D \right) \tilde{\Delta}_{2a}^{\pm}. \quad (5d)$$

## 2.2. Derivation of the critical pump parameters

The pump parameters  $\lambda_g$  and  $\lambda_a$  determine the respective strengths of the quantum coherent gain and absorption. The parameter  $\lambda_g$  must be sufficiently large to overcome the cavity and facet losses, while  $\lambda_a$  must be small enough so that the laser radiation can be sustained in the cavity. We will now derive the minimum pumping in the gain section,  $\lambda_{g,\min}$ , and the maximum pumping in the absorbing section,  $\lambda_{a,\max}$ , that are required to sustain stable pulses in the

cavity. At steady state, we can assume that the forward propagating electric field and the interaction with the medium will be the same as for the backward propagating electric field and the interaction with the medium. Therefore, we can write

$$\tilde{E}_+ = \tilde{E}_- = \tilde{E}, \quad (6a)$$

$$\tilde{\eta}_{g,a+} = \tilde{\eta}_{g,a-} = \tilde{\eta}_{g,a}, \quad (6b)$$

$$\tilde{\Delta}_{0g,a} = \tilde{\Delta}_{0g,a}, \quad (6c)$$

$$\tilde{\Delta}_{2g,a}^+ = \tilde{\Delta}_{2g,a}^- = \tilde{\Delta}_{2g,a}. \quad (6d)$$

At steady state, using  $\partial \tilde{\eta}_{g\pm} / \partial t = 0$  in Eq. (4b), the polarization in the gain section can be written as

$$\tilde{\eta}_g = i \frac{T_{2g}}{2} (\tilde{\Delta}_{0g} \tilde{E} + \tilde{\Delta}_{2g} \tilde{E}). \quad (7)$$

If we substitute  $\tilde{\eta}_g$  into Eq. (4a), we find the steady state electric field evolution in the gain section is given by

$$\left( \frac{\partial}{\partial z} + \frac{n}{c} \frac{\partial}{\partial t} \right) \tilde{E} = \frac{T_{2g}}{2} (\tilde{\Delta}_{0g} + \tilde{\Delta}_{2g}) \tilde{E} - l \tilde{E}. \quad (8)$$

Thus, the steady state gain is given by  $g = T_{2g}(\tilde{\Delta}_{0g} + \tilde{\Delta}_{2g})/2$ . At the lasing threshold, we can set

$$E_+ = E_- = 0, \quad (9a)$$

$$\tilde{\Delta}_{2g}^+ = \tilde{\Delta}_{2g}^- = 0. \quad (9b)$$

From Eq. (4c), we find  $\tilde{\Delta}_{0g} = \tilde{\lambda}_g T_{1g}$ , so that the small signal gain  $g_0$  in the gain section is given by  $g_0 = \tilde{\lambda}_g T_{1g} T_{2g} / 2$ . Analogously, we find that the quantum coherent absorption at steady-state is given by  $a = T_{2a}(\tilde{\Delta}_{0a} + \tilde{\Delta}_{2a})/2$  and the small-signal absorption is given by  $a_0 = \tilde{\lambda}_a T_{1a} T_{2a} / 2$ .

At threshold, the gain experienced by the propagating electric field in the gain section will have to be equal to the sum of the linear losses experienced by the propagating electric field in both the gain and absorbing sections, transmission losses at the two facets, and the resonant loss in the absorbing section. We can thus write

$$gL_g - aL_a - \left[ lL_c + \frac{1}{2} \ln \left( \frac{1}{r_1} \right) + \frac{1}{2} \ln \left( \frac{1}{r_2} \right) \right] = 0, \quad (10)$$

where  $L_g$  is the length of the gain section,  $L_a$  is the length of the absorbing section,  $L_c = L_g + L_a$  is the length of the cavity,  $r_1$  is the reflection coefficient of the first facet, and  $r_2$  is the reflection coefficient of the second facet. If there is no quantum coherent absorption, then we find

$$g_{\min} L_g - \left[ lL_c + \frac{1}{2} \ln \left( \frac{1}{r_1} \right) + \frac{1}{2} \ln \left( \frac{1}{r_2} \right) \right] = 0. \quad (11)$$

Therefore, the minimum pumping in the gain section to overcome the linear loss in the cavity and the losses in the two facets is

$$\lambda_{g,\min} = \frac{2}{T_{1g} T_{2g} L_g} \left[ lL_c + \frac{1}{2} \ln \left( \frac{1}{r_1} \right) + \frac{1}{2} \ln \left( \frac{1}{r_2} \right) \right]. \quad (12)$$

For a given gain coefficient  $g$ , the maximum value of the quantum coherent absorption that can sustain the pulse radiation is given by

$$a_{\max} L_a = gL_g - \left[ lL_c + \frac{1}{2} \ln \left( \frac{1}{r_1} \right) + \frac{1}{2} \ln \left( \frac{1}{r_2} \right) \right]. \quad (13)$$

Therefore, the maximum pumping coefficient in the absorbing section is given by

$$\lambda_{a,\max} = \lambda_g \frac{T_{1g}T_{2g}L_g}{T_{1a}T_{2a}L_a} - \frac{2}{T_{1a}T_{2a}L_a} \left[ lL_c + \frac{1}{2} \ln \left( \frac{1}{r_1} \right) + \frac{1}{2} \ln \left( \frac{1}{r_2} \right) \right]. \quad (14)$$

### 3. Results

We have simulated a two-section QCL that is shown schematically in Fig. 1. We assume that the gain section radiates light at  $6.2 \mu\text{m}$  and the absorbing section absorbs light at the same wavelength. The different parameter values of the active region and the cavity are given in Table 1. The parameter values in Table 1 are the same as the ones in [12, 16] so that we can compare our results with those presented in [12, 16] for actively modelocked QCLs. The parameter values in Table 1 apply for typical QCLs except  $T_1$ , which has been extended using a super-diagonal structure for modelocked operation. These parameters can be calculated for a designed QCL using the approaches as described in [18–21]. However, we have varied the key parameters, e.g., the recovery times  $T_{1g}$ ,  $T_{1a}$ , and the lengths of the gain and absorbing sections  $L_g$ ,  $L_a$  to show that they are not limiting parameters for creating stable ultra-short pulses.

Table 1. Key parameter values

Parameter	Symbol	Value
Recovery time in gain section	$T_{1g}$	50 ps
Recovery time in absorbing section	$T_{1a}$	50 ps
Coherence time in gain section	$T_{2g}$	0.05 ps
Coherence time in absorbing section	$T_{2a}$	0.05 ps
Ratio of absorbing to gain dipole moments	$d_a/d_g$	2
Length of cavity	$L_c$	2.6 mm
Length of gain section	$L_g$	2.3 mm
Linear loss	$l$	$10 \text{ cm}^{-1}$
Facet reflectivity	$r_1, r_2$	0.53
Diffusion coefficient	$D$	$4600 \times 10^{-12} \text{ mm}^2/\text{ps}$
index of refraction	$n$	3.2

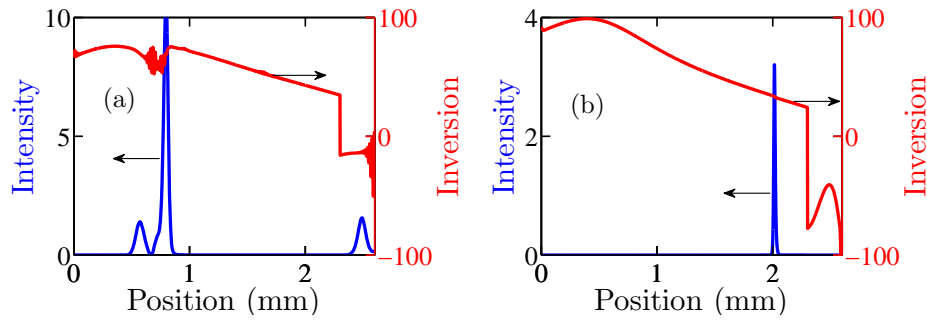


Fig. 2. Intensity and population inversion in the cavity after 100 round trips for (a)  $\lambda_g = 2.5\lambda_{g,\min}$  and  $\lambda_a = 0.3\lambda_{a,\max}$ , and (b)  $\lambda_g = 2.5\lambda_{g,\min}$  and  $\lambda_a = 0.7\lambda_{a,\max}$ .

In Figs. 2(a) and 2(b), we plot the light intensity, i.e.,  $E_+E_+^* + E_-E_-^*$ , and the population inversion, i.e.,  $\Delta = \Delta_0 + \Delta_2^+ \exp(2ikz) - \Delta_2^- \exp(-2ikz)$ , in the cavity. In Fig 2(a), the pumping

in the absorbing section  $\lambda_a$  is not enough to absorb the growing continuous waves from the gain section. Therefore, the driving terms on the right-hand side of Eqs. (4d) and (5d) are non-zero, which leads to oscillations of the population inversion due to spatial hole-burning. In Fig. 2(a), we note that the light intensity is spread over the cavity. By contrast, in Fig. 2(b), the pump coefficient in the absorbing section  $\lambda_a$  is enough to absorb the growing continuous waves from the gain section. Therefore, the driving terms on the right-hand side of Eqs. (4d) and (5d) are zero, and the population inversion does not oscillate. In Fig. 2(b), we note that the light intensity is confined over a very narrow spatial region in the cavity. This longitudinal spatial confinement leads to ultra-short, sub-ps light pulses in the output of the cavity.

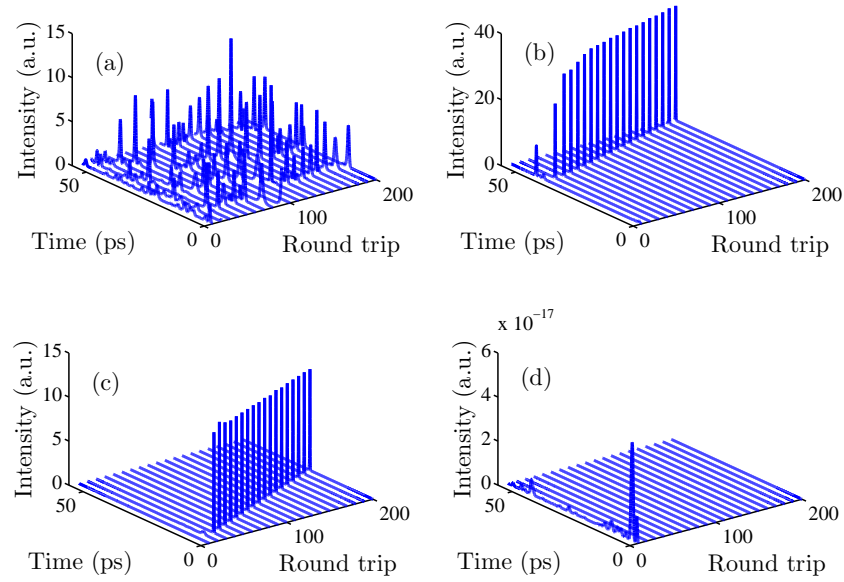


Fig. 3. Intensity output with  $\lambda_g = 2.5\lambda_{g,\min}$  and (a)  $\lambda_a = 0.3\lambda_{a,\max}$ , (b)  $\lambda_a = 0.6\lambda_{a,\max}$ , (c)  $\lambda_a = 0.9\lambda_{a,\max}$ , and (d)  $\lambda_a = \lambda_{a,\max}$ .

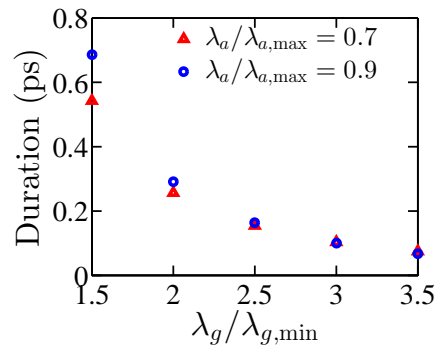


Fig. 4. Full width at half maximum (FWHM) duration of stable pulses with different pumping levels in the gain and absorbing sections.

In Fig. 3, we show the output intensities over 200 round-trips for a fixed  $\lambda_g$  as  $\lambda_a$  varies.

We note that ultra-short stable pulses are created when  $\lambda_a = 0.6\lambda_{a,\max}$  and  $\lambda_a = 0.9\lambda_{a,\max}$ . However, we observe a chaotic behavior when  $\lambda_a = 0.3\lambda_{a,\max}$ . We also note that the output intensity vanishes at  $\lambda_a = \lambda_{a,\max}$ . We have simulated the output intensity for different values of  $\lambda_g$ , and we have obtained similar results. In Fig. 3, we note that the pulses advance in time since the group velocity decreases due to the SIT effect [22, 23]. Since the pulse advances in time, the pulse repetition rate increases slightly from 18.058 GHz to 18.115 GHz, which may vary depending on the pump parameters.

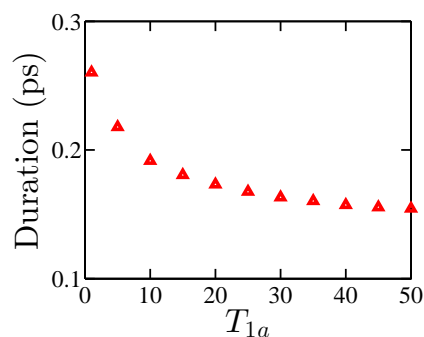


Fig. 5. Full width at half maximum (FWHM) duration of stable pulses with different recovery time in the absorbing section. The recovery time in the gain section is kept fixed at 50 ps.

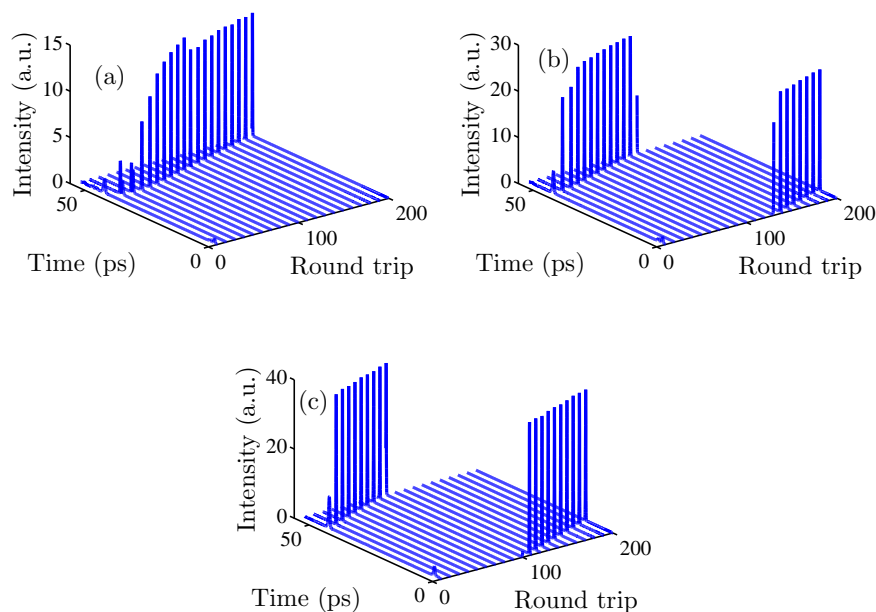


Fig. 6. Intensity output with  $\lambda_g = 2.5\lambda_{g,\min}$  and  $\lambda_a = 0.7\lambda_{a,\max}$  when (a)  $L_g = 2.0$  mm,  $L_a = 0.6$  mm, (b)  $L_g = 2.3$  mm,  $L_a = 0.3$  mm, and (c)  $L_g = 2.5$  mm,  $L_a = 0.1$  mm.

In Fig. 4, we plot the duration of the stable pulses for different pumping levels in the gain and absorbing sections. The pulse durations become smaller as the pumping in the gain section increases and the pumping in the absorbing section decreases. The pulse duration may be smaller than 100 fs. In Fig. 5, we plot the durations of stable pulses for different recovery times in the absorbing section and for a fixed recovery time in the gain section. We note that stable pulses are created even when  $T_{1a}$  is as short as 1 ps. The pulses become shorter as the recovery time in the absorbing section increases. We note that the Maxwell-Bloch equations solved in this work do not consider the saturable nonlinearity and group velocity dispersion that the pulse will experience while traveling in the cavity. However, these effects were extensively studied for SIT modelocked pulses in QCLs in [24]. It was found that stable modelocked pulses evolve over a broad parameter regime in the presence of nonlinearity and group velocity dispersion. In addition, the nonlinearity-induced changes are mostly canceled by the anomalous dispersion of typical QCLs and the stable pulse durations are not significantly changed.

In Fig. 6, we plot the pulse intensity evolution at the laser output with fixed pump parameters, but when the lengths of the gain and absorbing sections vary. We note that stable pulses are created in all cases. However, the pulse intensity increases and the pulse duration decreases as the length of the gain section increases and the length of the absorbing section decreases.

#### 4. Conclusion

We have proposed that stable ultra-short pulses can be created from a quantum cascade structure if the cavity is processed into two sections so that one section works as a gain medium and the other works as a resonant absorbing medium. This approach will allow one to control the pumping and bias-dependent parameters of the gain and absorbing periods separately, which should make it easier to construct a device than when gain and absorbing periods are interleaved. We have shown that in the proposed two-section QCL the saturable resonant absorbing section can suppress the growth of the continuous waves and the spatial hole-burning. Stable ultra-short pulses on the order of  $\sim 100$  fs are created when the pumping in the gain section is enough to overcome the losses in the cavity and the facets and the pumping in the absorbing section is less than the value that absorbs the light completely. The duration of the pulse can be varied by controlling the pumping parameters in the two sections.